Specific Surface Association of Avidin with *N*-Biotinylphosphatidylethanolamine Membrane Assemblies: Effect on Lipid Phase Behavior and Acyl-Chain Dynamics†

Musti J. Swamy‡ and Derek Marsh*

Abteilung Spektroskopie, Max-Planck-Institut für biophysikalische Chemie, 37070 Göttingen, Germany

Received December 22, 2000; Revised Manuscript Received September 5, 2001

ABSTRACT: The interaction of avidin with aqueous dispersions of *N*-biotinylphosphatidylethanolamines, of acyl chain lengths C(14:0), C(16:0), and C(18:0), was studied by using spin-label electron spin resonance (ESR) spectroscopy, ^{31}P nuclear magnetic resonance (^{31}P NMR) spectroscopy, differential scanning calorimetry, and chemical binding assays. In neutral buffer containing 1 M NaCl, binding of avidin is due to specific interaction with the biotinyl lipid headgroup because avidin presaturated with biotin does not bind. Saturation binding of the protein corresponds to a ratio of 50 lipid molecules per tetrameric avidin. Phospholipid probes spin-labeled at various positions between C-4 and C-14 in the *sn*-2 chain were used to characterize the effects of avidin binding on the lipid chain dynamics. In the fluid phase, protein binding results in a decrease of chain mobility at all positions of labeling while the flexibility gradient characteristic of a liquid-crystalline lipid phase is maintained. There is no evidence from the spin-label ESR spectra for penetration of the protein into the hydrophobic interior of the membrane. At temperatures corresponding to the gel phase, the lipid chain mobility increases on binding protein. The near constancy in mobility found with chain position, however, suggests that in the gel phase the lipid chains remain interdigitated upon binding avidin. Binding of increasing amounts of avidin results in a gradual decrease of the lipid chain-melting transition enthalpy with only small change in the transition temperature. At saturation binding, the calorimetric enthalpy is reduced to zero. ^{31}P NMR spectroscopy indicates that protein binding increases the surface curvature of dispersions of all three biotin lipids. The C(14:0) biotin lipid yields isotropic ^{31}P NMR spectra in the presence of avidin at all temperatures between 10 and 70 °C, in contrast to dispersions of the lipid alone, which give lamellar spectra at low temperature that become isotropic at the chain-melting temperature. In the presence of avidin, the C(16:0) and C(18:0) biotin lipids yield primarily lamellar ^{31}P NMR spectra at low temperature with a small isotropic component; the intensity of the isotropic component increases with temperature, and the spectra narrow and become totally isotropic at high temperature, in contrast to dispersions of the lipids alone, which give lamellar spectra in the fluid phase. The binding of avidin therefore reduces the cooperativity of the biotin lipid packing, regulates the mobility of the lipid chains, and enhances the surface curvature of the lipid aggregates. These effects may be important for both lateral and transbilayer communication in the membrane.

Molecular recognition at membrane surfaces involves the specific interaction of a membrane protein or lipid with an external ligand. The biological processes in which such recognition is involved include the stimulation of cell growth by binding of external growth factors to membrane receptors and regulation of ion channels by hormonal action, as well as situations in which lipids mediate interaction between external agents and the membrane, e.g., the various effects caused by the binding of lectins, toxins, viruses, and neurotransmitters to glycolipids (*1*). Detailed characterization of such systems is necessary to obtain an understanding of the underlying mechanisms. Studying model systems employing either naturally occurring or synthetic lipid membranes and proteins that can interact with the lipid headgroups is one possible starting point for such investigations.

The avidin−biotin system is an example of highly specific molecular recognition. The affinity of the egg-white protein avidin and the homologous protein streptavidin, isolated from *Streptomyces avidinii*, for the vitamin biotin is almost unparalleled in biology (*2, 3*). As a result of the high specificity and strength of interaction, this system has been exploited in many applications of biological and biomedical interest (for an overview, see ref *4*). In some of these cases, biotinylated phospholipids in which biotin is covalently linked to the amino function of phosphatidylethanolamine or phosphatidylserine are used (see, e.g., refs *5*−*7*). From the point of view of transmembrane communication, e.g., in the case of cholera toxin interaction with gangliosides, it is important to know what effects the binding of the protein ligand may have on the lipid receptor assembly. On the other hand, the effects of densely packed protein binding on the properties of the lipid membrane are of equal interest. For instance, it has been suggested that lipid sorting in the trans-Golgi may be linked to the targeting of GPI[1]-anchored proteins to the apical surface in polar epithelial cells (*8, 9*).

† This work was supported in part by the Deutsche Forschungsgemeinschaft.

* Corresponding author: Tel +49-551-201-1285; fax +49-551-201-1501; e-mail dmarsh@gwdg.de.

‡ Permanent address: School of Chemistry, University of Hyderabad, Hyderabad 500 046, India.

10.1021/bi0029189 CCC: $20.00 © 2001 American Chemical Society
Published on Web 11/15/2001

The binding of avidin to membranes composed of *N*-biotinylphosphatidylethanolamines (biotin-PEs) serves potentially as a model system for both these processes.

In the present paper, both spin-label electron spin resonance (ESR) and ^{31}P NMR as well as differential scanning calorimetry (DSC) studies on the interaction of avidin with biotin-PEs of acyl chain lengths C(14:0), C(16:0), and C(18:0) are presented. Calorimetry gives information on the cooperative behavior of the lipid assemblies; ESR spectroscopy reports on the lipid chain dynamics; ^{31}P NMR is sensitive to changes in the surface curvature of the lipid aggregates; and all three provide details of the different lipid states involved. It is found that the specific binding of avidin to the biotinyl moiety of the lipid headgroup not only abolishes the cooperativity of the chain melting (i.e., affects long-range communication) and perturbs generally lipid chain mobility but also gives rise to marked changes in the polymorphic phase behavior of the lipid assemblies.

MATERIALS AND METHODS

Materials. Avidin, DMPE, DPPE, and DSPE were purchased from Fluka (Buchs, Switzerland). Biotin *N*-hydroxysuccinimido ester was from Sigma (St. Louis, MO). Biotin-PEs were prepared from the corresponding PEs according to the method described in ref *5*. Phosphatidylcholine and phosphatidylethanolamine spin-labels, labeled at various positions along the *sn*-2 chain (*n*-PCSL and *n*-PESL, respectively) were synthesized according to the procedures described in ref *10*. *N*-Biotinylphosphatidylethanolamines, spin-labeled at positions 5 and 14 on the *sn*-2 chain (5-BPESL and 14-BPESL, respectively) were prepared from the corresponding spin-labeled PEs in a manner analogous to the synthesis of the unlabeled biotin-PEs.

Sample Preparation. For ESR measurements, 1 mg of DMBPE, DPBPE, or DSBPE and 1 mol % of the appropriate spin-labeled lipid probe were codissolved in CH_2Cl_2 and a thin film was formed by slow evaporation of the solvent under a stream of dry N_2 gas. The samples were vacuum-dried for at least 3 h before hydration with 100 μL of 10 mM Hepes buffer containing 1 mM EDTA. At this stage, the sample gave a clear solution, indicating that the lipid was in a micellar state. However, addition of NaCl from a 5 M stock solution in the same buffer to give a final salt concentration of 1 M resulted in a cloudy suspension of the lipid (see below). Recovery of the lipid when the thin film was hydrated with buffer containing 1 M NaCl was found to be difficult, and therefore in all experiments for ESR measurements the lipid film was first hydrated with buffer containing no salt and then the salt was added from a 5 M stock solution in the same buffer to yield the desired salt concentration. The hydrated samples were then transferred to 1 mm i.d. glass capillaries and pelleted in a benchtop microcentrifuge (Heraeus Biofuge) at 10 000 rpm. The excess supernatant was removed and the capillaries were flame-sealed before the ESR measurements. For experiments in which avidin binding was studied, the protein was added to the hydrated lipid dispersion from a 10 mg/mL stock solution of avidin in the same buffer. Alternatively, in some experiments the lipid film was hydrated directly with the protein solution. After incubation for at least 30 min at room temperature with intermittent mild vortexing, the samples were pelleted in a microcentrifuge. The pellet was washed twice with buffer and then transferred to a 1-mm i.d. glass capillary for ESR spectroscopy, prior to lipid/protein ratio determination. The supernatant and the washings were assayed for protein by measuring the absorbance at 282 nm. After ESR spectroscopy, the pellets were dissolved in a few drops of 0.5 M NaOH containing 5% SDS. Lipid/protein ratios were determined both from assay of the optical absorbance at 282 nm of the unbound protein in the supernatant [$\epsilon_{282}^{1\%,1cm} = 15.4$ OD (*2*)], as well as by estimation of protein and lipid phosphate in the pellet after ESR spectroscopy by using the methods of Lowry et al. (*11*) and Rouser et al. (*12*), respectively.

Samples for ^{31}P NMR spectroscopy were prepared by dissolving 20−30 mg of the lipid in dichloromethane, removing the solvent by rotary evaporation, and drying overnight under vacuum. The dried lipid was hydrated with 0.5 mL of 10 mM Hepes and 1 mM EDTA buffer, pH 7.4, at ca. 10° above the chain-melting transition temperature of the lipid. Avidin at a weight ratio to lipid of 1.2 was added from a concentrated stock solution, and after mild vortex mixing, the sample was transferred to a 10 mm NMR tube. For measurements in the presence of 1 M NaCl, salt was added from a 5 M stock solution to the sample without salt and the sample was vortex-mixed.

Samples prepared as for ^{31}P NMR spectroscopy were characterized morphologically by electron microscopy of specimens negatively stained with 1% aqueous uranyl acetate. For dispersions of DMBPE alone, no sizable structures were observed, consistent with these being optically clear micellar dispersions in the fluid phase. In the presence of avidin, the precipitated DMBPE dispersion consisted of large amorphous aggregates. No vesicular structures were observed. For dispersions of DSBPE alone, the sample consisted of large membranous sheets. In the presence of avidin, the DSBPE dispersion consisted of vesicular structures, with stain-excluding protein arrays visible on the surface in many cases. Vesicle size was somewhat heterogeneous, with the population of smaller vesicles having diameters in the region of 200 nm. Precise determination of the vesicle size distribution was not possible because of the aggregated nature of the sample.

ESR Spectroscopy. ESR spectra were recorded on a Varian E-9 E-line or an E-12 Century Line 9 GHz spectrometer equipped with a nitrogen-flow temperature regulation system. The sealed capillaries (1-mm diameter) were contained in a standard 4 mm diameter quartz tube containing silicone oil for thermal stability. Data were collected on a personal computer with analogue/digital interface using software written by Dr. M. D. King of this institute. Spectral

[1] Abbreviations: ESR, electron spin resonance; NMR, nuclear magnetic resonance; DSC, differential scanning calorimetry; PE, phosphatidylethanolamine; biotin-PE, *N*-biotinylphosphatidylethanolamine; DMBPE, DPBPE, and DSBPE, 1,2-dimyristoyl-, 1,2-dipalmitoyl-, and 1,2-distearoyl-*sn*-glycero-3-(*N*-biotinyl)phosphoethanolamine; DMPE, DPPE, and DSPE, 1,2-dimyristoyl-, 1,2-dipalmitoyl-, and 1,2-distearoyl-*sn*-glycero-3-phosphoethanolamine; *n*-PCSL and *n*-PESL, 1-acyl-2-[*n*-(4,4-dimethyloxazolidine-*N*-oxyl)]stearoyl-*sn*-glycero-3-phosphocholine and -phosphoethanolamine; *n*-BPESL, 1-acyl-2-[*n*-(4,4-dimethyloxazolidine-*N*-oxyl)]stearoyl-*sn*-glycero-3-(*N*-biotinyl)phosphoethanolamine; CSA, chemical shift anisotropy; EDTA, ethylenediaminetetraacetic acid; Hepes, *N*-(2-hydroxyethyl)piperazine-*N*′-2-ethanesulfonic acid; GPI, glycosylphosphatidylinositol; SDS, sodium dodecyl sulfate.

subtractions were performed interactively on a personal computer with software written by Dr. J. Kleinschmidt of this laboratory.

Differential Scanning Calorimetry. DSC measurements were performed on a Hart Scientific Model 4207 heat-flow calorimeter. Lipid samples were weighed into the ampules, 0.1 mL of the buffer (10 mM Hepes and 1 mM EDTA, pH 7.4) was added, and the ampules were sealed tightly with the screw caps. Complete hydration was ensured by heating the ampules above the phase transition temperature in the calorimeter. The samples were then allowed to cool to room temperature, protein solution in the same buffer was added to yield the desired lipid/protein ratio, and the sample was mixed by drawing several times into a Pasteur pipet. NaCl was then added from a 5 M stock solution to give a final concentration of 1 M and the sample volume was adjusted to 0.5 mL by addition of the appropriate amount of buffer. Experiments were also performed by adding the NaCl stock solution first, followed by addition of the protein. The ampules were then sealed with the screw caps and vortexed to achieve homogeneous mixing. Samples first were incubated at 37 °C for 2 h in the calorimeter and then for 1 h at 1 °C, to achieve proper equilibration before data acquisition. The scan rate was 10°/h. The reference cell contained an empty ampule for all the experiments, and baselines, obtained from samples containing the same volume of buffer alone, were subtracted from the experimental data. After the experiments, the samples were recovered from the ampules and centrifuged at 10 000 rpm for 10 min in a benchtop microcentrifuge. The supernatants were assayed for unbound protein by monitoring the absorbance at 282 nm. The pellets were dissolved in 0.5 M NaOH containing 5% SDS and the lipid-to-protein ratios were determined as described above for the ESR samples.

^{31}P Nuclear Magnetic Resonance Spectroscopy. Proton-dipolar decoupled ^{31}P NMR spectra were recorded at a frequency of 121.5 MHz on a Bruker MSL 300 spectrometer operating in the Fourier transform mode. The $\pi/2$ pulse width was 11 μs and recycle delays were always in excess of $5T_1$. The decoupling power was in the range of 10−15 W and the duty cycle of the gated decoupling was approximately 0.2%.

RESULTS

Avidin Binding Assays. Binding of avidin to the three biotin-PEs, namely, DMBPE, DPBPE, and DSBPE, was determined by adding the protein to the lipid dispersions in 10 mM Hepes buffer containing 1 M NaCl and 1 mM EDTA, pH 7.4. The binding of avidin to the lipid dispersion resulted in the rapid formation of large precipitated aggregates. The binding curve for association of avidin with DMBPE dispersions is given in Figure 1. At low protein-to-lipid ratios, all the avidin added was bound to the lipid. At saturation binding, the lipid/protein ratio was 50 lipids bound/protein tetramer. This indicates that, at saturation, only about 4−8% of the biotin moieties attached to the lipid headgroups would be bound specifically by avidin. Washing the pellet did not result in any loss of protein, indicating that the binding is very tight. Assay of the number of sites still available for binding of biotin in the avidin/biotin-PE pellets at saturation protein binding (by using spin-labeled free biotin) revealed that this was <1 per avidin tetramer. Protein binding was due to the specific interaction of avidin with the biotinyl moiety of the lipids because avidin presaturated with biotin did not bind to the lipid. These and all subsequent experiments were performed in buffers containing 1 M NaCl in order to eliminate nonspecific electrostatic binding of this basic protein to the negatively charged lipids.

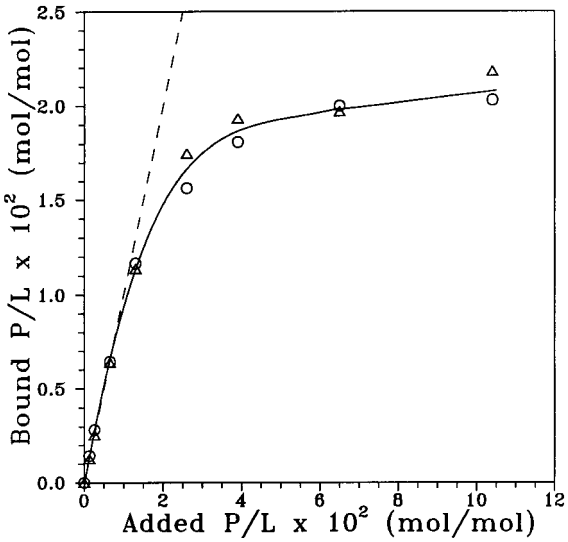

FIGURE 1: Dependence of avidin binding to DMBPE dispersions on the total protein/lipid ratio of avidin added. Buffer: 10 mM Hepes, 1 M NaCl, and 1 mM EDTA, pH 7.4. The dashed line corresponds to complete binding of the added avidin. Data are obtained from analysis of the lipid/protein pellet (○) and of recovery in the supernatant (△) and are given as the mole ratio (P/L) of avidin tetramer to DMBPE lipid.

Spin-Label ESR Spectroscopy. The ESR spectra of the 5-PCSL spin-label in dispersions of DMBPE, DPBPE, and DSBPE in the absence as well as in the presence of avidin bound at saturation are shown in Figure 2. Spectra shown were recorded at temperatures in the gel phase as well as in the fluid phase of the biotinyl lipid dispersions.Very marked changes in the spectra of 5-PCSL result from binding avidin to the biotin-PE host lipid. At temperatures in the gel phase of the biotin lipid (Figure 2a−f), the outer hyperfine splitting is decreased on binding avidin, whereas at temperatures corresponding to the fluid phase of the lipid (Figure 2g−l), it is increased. The temperature dependence of the outer hyperfine splitting constant, A_{max}, of the 5-PCSL spin-label in DMBPE dispersions in 1 M NaCl in the absence and in the presence of different concentrations of avidin is given in Figure 3A. Addition of protein results in an increase in the outer hyperfine splitting throughout the entire fluid phase and in a decrease in A_{max} throughout the entire gel phase. These opposite effects are accompanied by attenuation of the phase transition on binding avidin such that at saturating concentrations (5:1 w/w ratio of added avidin) the chain-melting transition of the lipid is totally abolished. Corresponding data for the longer-chain DPBPE and DSBPE lipids in the presence and absence of avidin are given in Figure 3B. Protein binding has a similar effect on these two biotin lipids, in that A_{max} is also decreased in the gel phase and increased in the fluid phase, and the phase transitions are nearly abolished at a ratio of 5:1 (w/w) avidin added. (In 1 M NaCl, DPBPE and DSBPE are lamellar in both gel and fluid phases; see ref *14*.) Thus, for all three lipids, abolition of the lipid phase transition results from an increased mobility

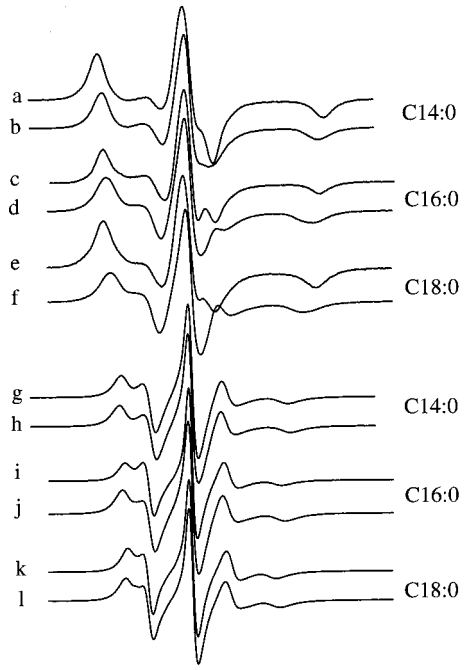

FIGURE 2: ESR spectra of the 5-PCSL phosphatidylcholine spin-label in dispersions of C(14:0), C(16:0), and C(18:0) biotin-PE, in the presence and in the absence of avidin. Buffer: 10 mM Hepes, 1 M NaCl, and 1 mM EDTA, pH 7.4. (a−f) Spectra recorded in the gel phase; (g−l) spectra recorded in the fluid phase. (a, b) DMBPE at 2 °C; (c, d) DPBPE at 20 °C; (e, f) DSBPE at 30 °C; (g, h) DMBPE at 40 °C; (i, j) DPBPE at 52 °C; and (k, l) DSBPE at 66 °C. The upper spectrum in each pair is for the lipid alone and the lower spectrum is for the lipid saturated with bound avidin (5:1 w/w added). Spectral width: 100 G.

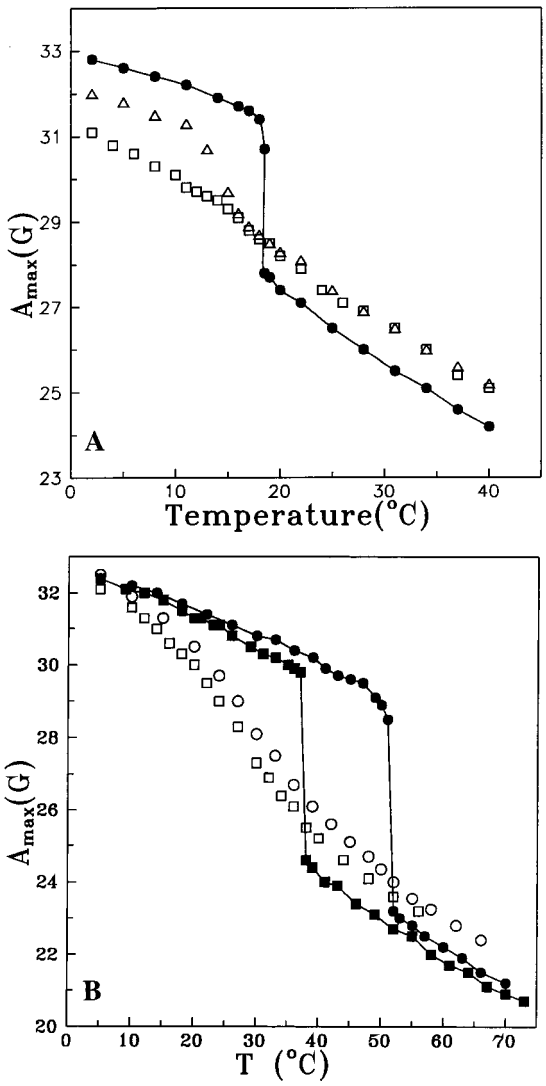

FIGURE 3: Temperature dependence of the outer hyperfine splitting, A_{max}, for the 5-PCSL phosphatidylcholine spin-label in dispersions of biotin-PEs of different chain lengths. (A) DMBPE dispersions in the absence (●) and in the presence of 3:1 w/w (△) and 5:1 w/w (□) added avidin. (B) DPBPE (■, □) and DSBPE (●, ○) dispersions in the absence (filled symbols) and in the presence (open symbols) of 5:1 (w/w) added avidin. Buffer: 10 mM Hepes, 1 M NaCl, and 1 mM EDTA, pH 7.4.

of the lipid molecules in the gel phase due to perturbations in the cooperativity of lipid chain packing caused by protein binding, and correspondingly a hindering of the lipid chain mobility in the fluid phase due to the interaction of the lipid headgroups with the protein.

The ESR spectra of different phosphatidylcholine spin-label positional isomers (*n*-PCSL, $n = 4$, 8, 10, and 14) in DMBPE dispersions both in the presence and in the absence of saturating amounts of avidin (5:1 w/w added protein) are shown in Figure 4. These spectra were recorded at a fixed temperature corresponding to the gel phase of the lipid alone. Apart from some spin−spin broadening for 10-PCSL, the spectra of the various *n*-PCSL labels in the DMBPE gel phase are all very similar in the absence of avidin. This corresponds to the formation of an interdigitated L_{β}^{i} gel phase (*13*). In contrast, the different spin-label positional isomers evidence a slight but progressively increasing segmental mobility with position down the lipid chain upon binding avidin. Interestingly, the spectrum of 14-PCSL consists of two components even at 2 °C, in the presence of avidin (Figure 4h). The temperature dependence of this spectrum is given in Figure 5. Two coexisting spectral components are observed at least up to 25 °C. For the 12-PCSL positional isomer, two spectral components are also observed in the presence of avidin but are first resolved at a temperature higher than 2 °C (data not shown). Also with the 10-PCSL positional isomer, two-component spectra are resolved over a limited temperature range in the presence of avidin.

Corresponding ESR spectra of the different *n*-PCSL positional isomers in DMBPE dispersions, at a temperature corresponding to the fluid phase of the lipid alone, are given in Figure 6. The spectral anisotropy and outer hyperfine splittings are consistently higher in the presence of avidin than in its absence, at all positions of chain labeling. The dependence of the outer hyperfine splitting constant, A_{max}, on label position in the *sn*-2 chain of *n*-PCSL is given in Figure 7 for DMBPE dispersions at low and high temperatures, in both the presence and absence of avidin. Whereas the positional dependence is relatively small at 2 °C, corresponding to the gel phase of DMBPE, a profile of increasing chain flexibility is seen at 40 °C in the fluid phase. At saturation binding of avidin, this chain flexibility gradient that is characteristic of the fluid phase is preserved. The sole difference is that the values of A_{max} in the fluid phase are consistently higher at all chain positions in the presence of excess avidin.

Differential Scanning Calorimetry. Differential scanning calorigrams obtained on heating dispersions of DMBPE alone

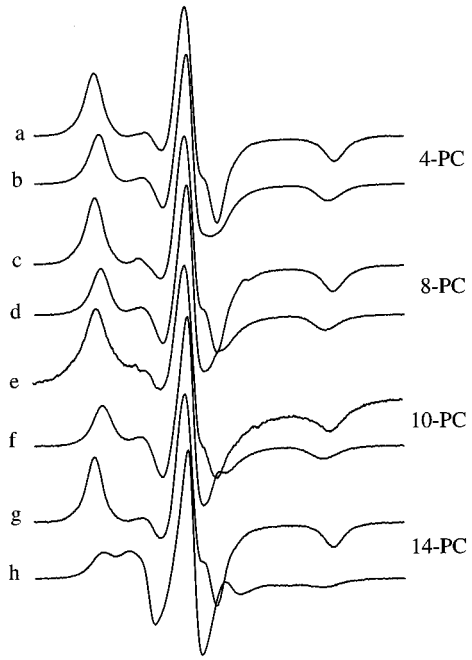

FIGURE 4: ESR spectra at 2 °C of phosphatidylcholine spin-label positional isomers, *n*-PCSL, in DMBPE dispersions in the absence and in the presence of 5:1 w/w added avidin. Buffer: 10 mM Hepes, 1 M NaCl, and 1 mM EDTA, pH 7.4. (a, b) 4-PCSL; (c, d) 8-PCSL; (e, f) 10-PCSL; (g, h) 14-PCSL. The upper spectrum in each pair is for the lipid alone and the lower spectrum is for the lipid saturated with bound avidin. Spectral width: 100 G.

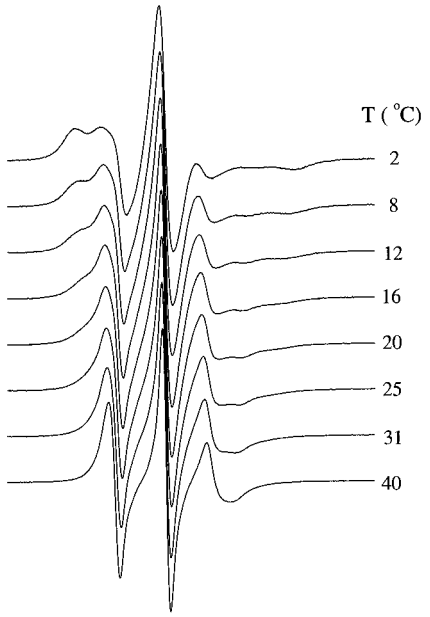

FIGURE 5: Temperature dependence of the ESR spectra of the 14-PCSL spin-label in DMBPE dispersions with bound avidin (5:1 w/w added). Spectral width: 100 G.

and those to which avidin was bound at various lipid/protein ratios are given in Figure 8. For each endotherm shown, the data were normalized to 1 mg of lipid, to facilitate direct comparison. For clarity, the traces are also displaced vertically. From Figure 8, it can be seen that the transition enthalpy decreases progressively with increasing protein binding, with only very slight effect on the position of the transition. The transition enthalpy is given as a function of

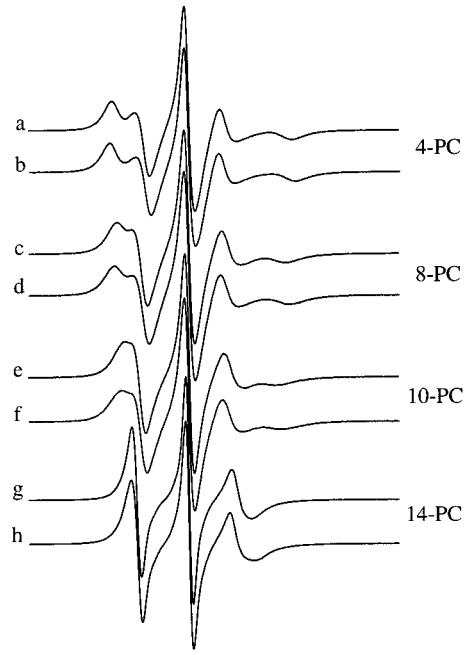

FIGURE 6: ESR spectra at 40 °C of phosphatidylcholine spin-label positional isomers, *n*-PCSL, in DMBPE dispersions in the absence and in the presence of 5:1 (w/w) added avidin. Buffer: 10 mM Hepes, 1 M NaCl, and 1 mM EDTA, pH 7.4. (a, b) 4-PCSL; (c, d) 8-PCSL; (e, f) 10-PCSL; (g, h) 14-PCSL. The upper spectrum in each pair is for the lipid alone and the lower spectrum is for the lipid with bound avidin. Spectral width: 100 G.

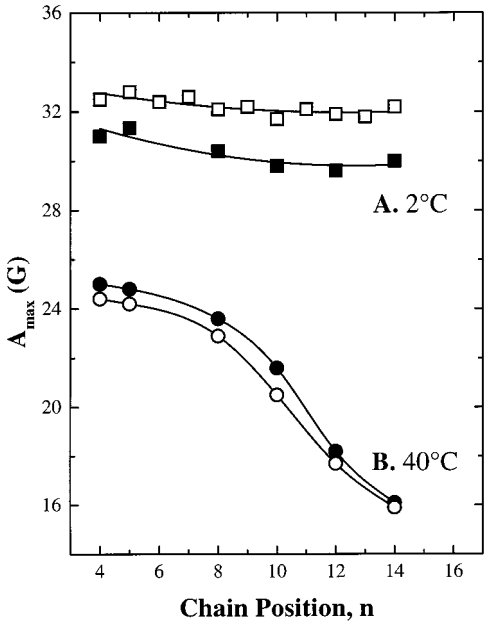

FIGURE 7: Outer hyperfine splitting, A_{max}, at (A) 2 °C and (B) 40 °C as a function of nitroxide position, *n*, in the *sn*-2 chain for the *n*-PCSL phosphatidylcholine spin-label positional isomers in DMBPE dispersions in the absence (open symbols) and in the presence (filled symbols) of 5:1 (w/w) added avidin. Buffer: 10 mM Hepes, 1 M NaCl, and 1 mM EDTA, pH 7.4.

the protein/lipid ratio of avidin bound in Figure 9. The decrease in transition enthalpy, ΔH_t, depends approximately linearly on the ratio of avidin bound/lipid and is reduced to zero at a level of binding corresponding to ca. 50 lipids/avidin tetramer. The above data correspond to experiments in which the protein was added before the addition of salt.

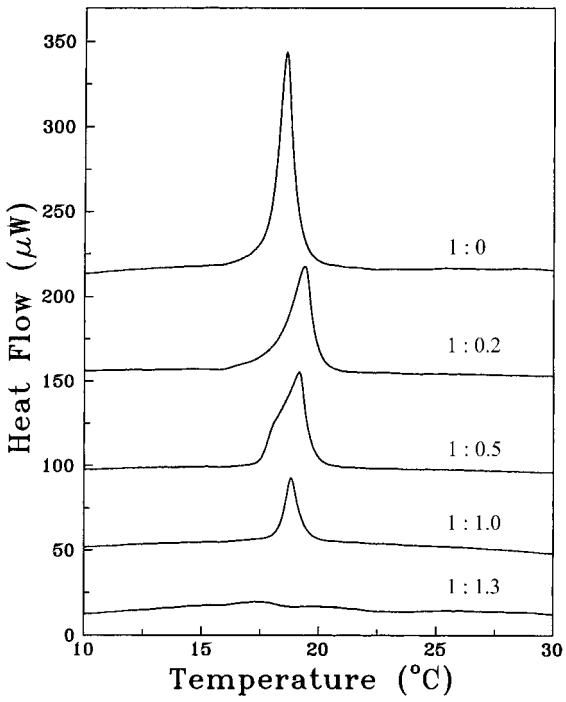

FIGURE 8: Differential scanning calorigrams (heating rate 10°/h) of DMBPE in the presence of increasing amounts of avidin. From top to bottom, the endotherms correspond to lipid alone and lipid−protein mixtures at weight ratios of 1:0.2, 1:0.5, 1:1.0, and 1:1.34, respectively. Buffer: 10 mM Hepes, 1 M NaCl, and 1 mM EDTA, pH 7.4.

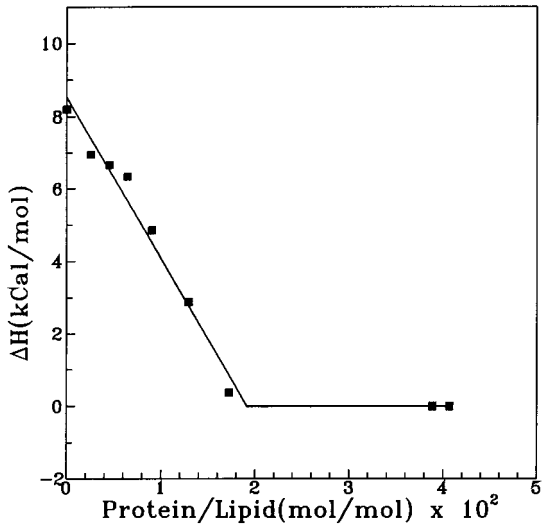

FIGURE 9: Dependence of the chain-melting transition enthalpy, ΔH_t, of DMBPE dispersions on the protein/lipid ratio of avidin bound. The last two data points correspond to the (excess) amount of avidin added. The sloping part of the solid line represents a least-squares fit to the first seven data points. Buffer: 10 mM Hepes, 1 M NaCl, and 1 mM EDTA, pH 7.4.

Experiments in which protein was added after the addition of salt similarly indicated that the transition enthalpy decreases with increasing protein binding (data not shown). However, it was found that equilibration was achieved rather slowly in such experiments, and therefore these experiments were not pursued in detail.

^{31}P NMR Spectroscopy. In 1 M NaCl, DMBPE, DPBPE, and DSBPE all form interdigitated gel phases at low temperatures where they give ^{31}P NMR spectra characteristic of lamellar gel phases (*14*). The fluid phases in the presence of 1 M NaCl as seen by ^{31}P NMR spectroscopy are, however, different for each of the three lipids. To investigate the effect of avidin binding on these different structures, proton-dipolar decoupled, broad-line ^{31}P NMR spectra were recorded in the presence of avidin (1.2:1 w/w) for dispersions of the three biotin-PEs of different chain lengths in 1 M NaCl. The ^{31}P NMR spectra for dispersions of the three lipids in the presence of avidin are shown in Figure 10. In the presence of avidin, the spectra from DMBPE dispersions consist of a single isotropic line, the width of which decreases with increasing temperature. For both DPBPE and DSBPE dispersions, however, the ^{31}P NMR spectra at low temperature in the presence of avidin consist primarily of axially symmetric lamellar powder patterns, with a small isotropic component superimposed. With increasing temperature, the proportion of the isotropic component increases progressively and at high temperature the spectra consist solely of a single, sharp isotropic line. In the absence of avidin, both these lipids give ^{31}P NMR spectra characteristic of fluid lamellar phases at high temperature (*14*).

DISCUSSION

The specific interaction of avidin with three biotin-PEs of hydrocarbon chain lengths C(14:0), C(16:0), and C(18:0) in aqueous dispersions with 1 M NaCl, and the resulting effects on their chain mobility, phase transitions, and polymorphic phase behavior have been studied by using spin-label ESR spectroscopy, ^{31}P NMR spectroscopy, and differential scanning calorimetry. The results indicate that protein binding progressively attenuates the chain-melting phase transition of the lipid. Concomitantly, the lipid chain mobility is increased in the gel phase and decreased in the fluid phase. The induction by avidin binding of more isotropic structures in the lamellar lipid membranes could be important as a model system for other systems involving headgroup-specific lipid−protein interactions. The mode of surface association of avidin and the effects of this interaction on the different properties of the lipid dispersions are discussed in detail separately below.

Avidin Binding Stoichiometry. The binding of avidin to aqueous dispersions of biotin-PEs in 1 M NaCl that is studied here corresponds to the specific interaction with the biotinylated lipid headgroups, because presaturation with biotin abolishes binding completely. In 1 M NaCl, screening of the surface electrostatics of the negatively charged biotin lipids prevents the nonspecific absorption that is observed at low ionic strength (cf. ref *15*). The binding curve of avidin with DMBPE dispersions (Figure 1) evidences complete binding of the added protein at lower avidin concentrations, but complete binding is not maintained as the amount of avidin added approaches saturation binding level. Because the binding of biotin to avidin is of extremely high affinity (*2*), this inhibition of binding must arise from steric exclusion at higher degrees of coverage of the lipid surface by avidin.

The saturation level of avidin binding determined at a 5:1 weight ratio of added protein to lipid corresponds to a stoichiometry of 50 DMBPE molecules/avidin tetramer. This value can be compared with the dimensions of the homologous streptavidin (*16*), whose X-ray crystal structure is known (*17*, *18*). The core streptavidin tetramer measures 54

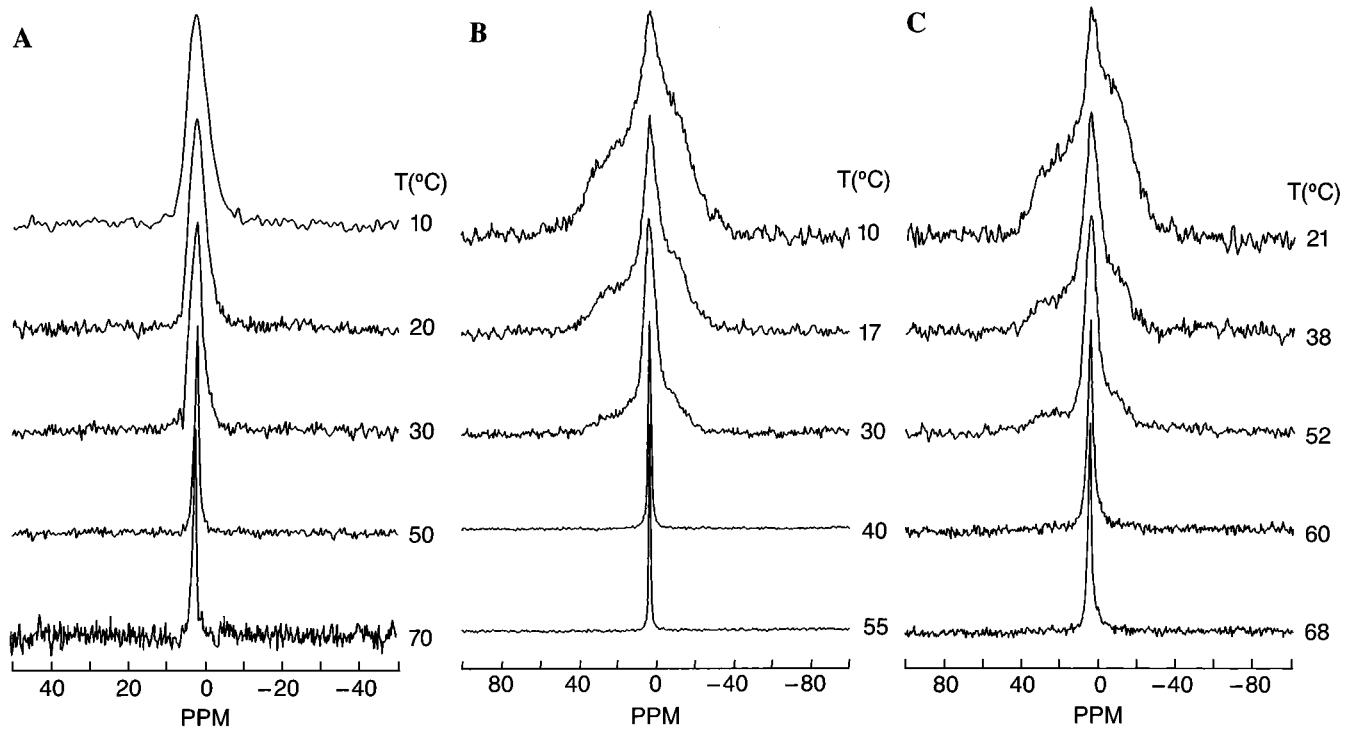

FIGURE 10: Proton-dipolar decoupled 121.5 MHz ^{31}P NMR spectra of biotin-PEs of different chain lengths dispersed in 10 mM Hepes buffer, 1 M NaCl, and 1 mM EDTA, pH 7.4, in the presence of avidin (1.2:1 w/w). The temperature at which each spectrum was recorded is indicated in the figure. (A) DMBPE, (B) DPBPE, (C) DSBPE. Chemical shifts are referenced to external 85% phosphoric acid.

× 58 × 48 Å along the three molecular axes *P*, *Q*, and *R* (*17*). The dimensions of the tetramer of deglycosylated avidin (50 × 56 × 40 Å) are somewhat smaller (*19*). There are two biotin binding pockets at opposite faces of the tetramer that are located in each case at one end of the monomer β-barrel structure. When the protein binds to the biotinyl moieties of the lipid molecules, at least one *P* × *R* plane (with two binding sites) is expected to be adjacent to a membrane surface (*20*). Assuming an area per lipid molecule of 80−90 Å^2, corresponding to the interdigitated gel phase and the more expanded fluid phase, respectively (cf. ref *14*), a binding stoichiometry of 55−65 lipid molecules/protein tetramer is predicted at complete surface coverage with cross-bridging between two lipid layers. Similar values are obtained from the projection (∼ 55 × 45 Å) of the streptavidin tetramer on the membrane plane in 2-D crystals (*21*). Corresponding values for the deglycosylated avidin, deduced from 3-D crystals (*19*), are approximately 40−50 lipids/tetramer. These estimates (i.e., ∼50 lipids/tetramer) are in reasonable agreement with the avidin binding stoichiometry measured here. It appears, therefore, that saturation binding of avidin corresponds to complete coverage of the biotin lipid surface and that the avidin tetramer cross-links between adjacent lipid layers. Evidence for the latter comes from the fact that the biotin lipid dispersion precipitates completely on the addition of avidin, and also that only a very small number of binding sites were available to free biotin in the avidin/biotin lipid complexes. At this saturation level of protein binding, only 4−8% of the biotin lipid headgroups are specifically complexed by avidin; further binding is prevented for steric reasons. Nevertheless, at this same level the lipid chain-melting phase transition is totally eliminated.

Effect of Avidin Binding on the Lipid Mobility and Thermotropic Phase Behavior. As seen for DMBPE, avidin binding decreases the transition enthalpy of the biotin-PEs and also broadens the chain-melting phase transition considerably (Figure 8). The transition width increases progressively with increasing concentration of bound protein and finally, at saturation binding, no phase transition could be detected (Figure 9). As can be seen from Figure 3, binding increases the lipid mobility in the gel phase but decreases it in the fluid phase.

The removal of the cooperative lipid chain melting is almost certainly mediated by disruption of the long-range interactions between lipids by those lipids that are specifically bound to avidin. It was shown previously that the biotin lipids bound to avidin are partly drawn up out of the bilayer (*22*, *23*). This vertical dislocation will certainly disrupt the cooperativity of the lipid assemblies. At saturation binding, two biotin lipids in every 50 are specifically bound to avidin at spatially separated sites (see previous subsection). Therefore this should be sufficient to limit the cooperativity of interactions in the gel-phase lipid matrix.

From Figure 7, it can be seen that, for the free lipid as well as for the lipid−protein complexes, the values of A_{max} obtained at 2 °C are nearly constant as the nitroxide spin-label position is stepped down the *sn*-2 chain of the phosphatidylcholine from C-4 to C-14. For normal bilayer structures, it has been shown previously that, even in the gel phase, the values of A_{max} obtained for nitroxide spin-labels close to the terminal methyl ends of the acyl chains are considerably smaller than those obtained for spin-labels located closer to the lipid headgroup. However, for lipids with interdigitated chains, the mobility of nitroxide spin-labels close to the methyl ends of the hydrocarbon chains is similar to that close to the glycerol backbone (*24*, *25*). X-ray diffraction studies (*14*) on C(14:0)−C(18:0) biotin-PEs have shown that they exhibit chain interdigitation in the gel phase,

in agreement with the ESR data for DMBPE alone in Figure 7A. The ESR results for samples in the presence of protein indicate that, even after binding of avidin, the biotin lipid appears to retain its chain interdigitation and lamellar structure at low temperatures.

It is interesting to note that the spectrum of 14-PCSL at 2 °C exhibits two components in DMBPE in the presence of avidin (see Figure 4h). Also, a biotin-PE spin-label, labeled at the 14-position of the *sn*-2 chain (14-BPESL), gives similar two-component spectra under the same conditions (spectra not shown). In addition to the rigid component, which is expected at this low temperature, there is also a more mobile component. This latter component of intermediate mobility is also present at higher temperatures (but below the chain-melting transition temperature of the lipid—above the transition temperature there is only a single spectral component; Figure 5). While a final explanation cannot be given for the presence of two components, it is unlikely to be due to a penetration of the protein into the hydrophobic interior of the membrane because in the gel phase (with interdigitated chains) the nitroxide moiety of 14-PCSL should be near the polar headgroup region of the opposing surface of the bilayer. The most likely explanation for the two components is that, in the gel phase, avidin can perturb the lipids in the immediate vicinity of that lipid to whose headgroup it binds specifically. In the fluid phase, the lipid is no longer in an interdigitated state, and because the lipid chain packing is no longer so highly cooperative as it is in the gel phase, the ESR spectra of the spin-labels at the 14-position do not display two components upon protein binding.

Effect of Avidin Binding on the Polymorphic Lipid Phase Behavior. ^{31}P NMR spectra reflect diagnostically the surface curvature in phospholipid aggregates. Isotropic spectra indicate highly curved surfaces such as those from micelles, small unilamellar vesicles, and bicontinuous cubic phases. Structures with cylindrical symmetry give spectra with a positive chemical shift anisotropy (CSA), which is reduced in magnitude relative to lamellar systems, and multilamellar vesicles or large unilamellar vesicles yield spectra with a negative CSA (*26*,*27*). In the absence of avidin, all three biotin-PEs used in this study form interdigitated bilayer structures in the gel phase and give ^{31}P NMR spectra characteristic of a lamellar gel phase (*14*). The corresponding fluid phases of these three lipids in 1 M NaCl, however, differ in their structures as recorded by ^{31}P NMR spectroscopy. DMBPE yields isotropic spectra, indicating highly curved surfaces, and DSBPE gives spectra with a negative CSA that are characteristic of a fluid lamellar phase. The ^{31}P NMR spectra of the intermediate chain length analogue, DPBPE, display a more complex behavior in the fluid phase, changing from a pattern that has a small negative CSA at temperatures immediately above the chain-melting phase transition to one that is characteristic of a normal fluid lamellar phase at high temperature (*14*). Previous morphological observations (*14*) and those given here for negatively stained specimens are substantially in agreement with this characterization by ^{31}P NMR.

Because the three biotin lipids differing only in their acyl chain length show such dramatic differences in the structure of their fluid phases, it is of considerable interest to examine the effect of protein binding on these different structures. In the presence of avidin, the spectra of DMBPE in 1 M NaCl are isotropic throughout the temperature range studied (from 10 to 70 °C), whereas for both DPBPE and DSBPE dispersions with avidin, the spectra convert gradually from a lamellar pattern at low temperature in the gel phase to an isotropic pattern at high temperature (see Figure 10). It therefore appears that, in the presence of avidin, the membranes of DMBPE are highly curved even at low temperatures, whereas the curvature of DPBPE and DSBPE membranes in the presence of avidin increases with increasing temperature. Alternatively, because lipid translational diffusion rates increase with increasing temperature, the same system that gives anisotropic spectra at low temperature may yield isotropic spectra at high temperature. However, if the latter is the case, the structures formed at low temperature in the presence of avidin must be different from those formed by the lipid dispersions alone, because otherwise an increase in translational diffusion rate could not by itself bring about the spectral changes found in the presence of the protein. Thus, in either case, it is clear that avidin binding can have a profound effect on the surface curvature of the biotin-PE dispersions.

The ^{31}P NMR observations on the avidin/biotin lipid complexes can be further interpreted in terms of the morphological characterization that is given in the Materials and Methods section. The amorphous aggregates of DMBPE observed in the presence of avidin most likely consist of small micellar structures to which avidin is bound. Reference to the ^{31}P NMR spectra given in Figure 10A suggests these aggregated structures are preserved over the temperature range studied (cf. also Figure 3A). Translational diffusion of the phospholipids around the surface of the highly curved micelles gives rise to the isotropic averaging of the ^{31}P chemical shift anisotropy. (Note that only a small percentage of the biotin lipid is bound by avidin. Therefore nearly all lipids will undergo unrestricted translational diffusion.) Increasing temperature enhances the rate of lateral diffusion resulting in the progressive line narrowing that is seen in Figure 10A. This parallels the gradual increase in lipid chain mobility with increasing temperature (with no cooperative gel-phase formation) that is shown for avidin/DMBPE complexes in Figure 3A.

A similar explanation holds for the temperature dependence of the ^{31}P NMR spectra of the DSBPE dispersions to which avidin is bound (Figure 10C). These samples are also aggregated and therefore lipid translational diffusion, and not vesicle rotation, is the origin of the observed temperature-dependent motional narrowing. In contrast to DMBPE in the presence of avidin, however, the avidin-bound DSBPE complexes are larger and vesicular. Therefore, isotropic averaging is not achieved at low temperature and only becomes complete at temperatures in the region of 60 °C and higher (see Figure 10C). At 21 °C, translational diffusion is insufficient to average the ^{31}P CSA that is characteristic of the lamellar vesicles observed by electron microscopy. Only a minor population of vesicles are sufficiently small to produce the residual isotropic peak.

Order of magnitude estimates support this interpretation of the ^{31}P NMR spectra for the vesicular DSBPE/avidin complexes. The mean square distance travelled by 2-D translational diffusion in time t is given by $\langle d^2 \rangle = 4D_T t$, where D_T is the translational diffusion coefficient. In a spherical vesicle, the area covered that corresponds to a solid

angle of 1 steradian is $\langle d^2 \rangle \sim R^2$, where R is the radius of the vesicle. For the smallest vesicle population, $R \sim 90$ nm. With a translation diffusion coefficient of $D_T \sim 10^{-7}$ cm•s^{-1} that is characteristic of fluid bilayers (*28*), this gives an inverse time-of-flight of $t^{-1} \sim 5$ kHz. For comparison, the CSA of the lamellar phase is ~45 ppm and at a Larmor frequency of 121 MHz this corresponds to a frequency dispersion of ~5.5 kHz. This is therefore reasonably consistent with the population of smallest vesicles producing an isotropic resonance, and the larger vesicles being of such a size that motional averaging occurs only at high temperatures.

Thus the DSBPE lipid forms lamellar membranes in both the presence and absence of avidin. However, a change in morphology is induced by the binding of avidin. This results in the formation of more highly curved, vesicular membranes, as opposed to the large membranous sheets into which DSBPE assembles in high salt in the absence of avidin (*14*).

Implications. In addition to the obligatory interactions of proteins of the conventional integral and peripheral classes with membrane lipids, there is a third class of lipid−protein interaction, which is exemplified by the systems that have been studied here. This third category consists of proteins that interact selectively with the headgroups of specific lipid molecules. Such proteins include lectins, toxins such as the cholera toxin, hormones, and neurotransmitters, all of which can interact with glycolipid headgroups. The biological properties of these proteins are generally supposed to be mediated by the interaction with their receptor lipids. However, details of the mechanisms are, in most cases, not yet clear. The present study on the interaction of avidin with the biotin-PEs serves as a model system for such interactions. For example, it is known that surface binding of certain proteins to their specific cell-surface receptors induces changes in their biological properties, e.g., the mitogenic activation of lymphocytes by lectins (*29*). Among other effects, the induction of more isotropic structures in the biotin-PE membranes by avidin binding suggests that possible mechanisms in such processes could involve local changes in the lipid phase structure induced by protein binding, in addition to the modulation of the lipid cooperativity and dynamics. Several membrane-bound enzymatic and channel activities are known to be modulated by lipids that affect membrane curvature (*30*, *31*). Here, such changes are brought about instead by protein binding to a receptor lipid. Last but not least, specific binding at relatively dilute sites (one per 50 lipids) influences the long-range cooperative lipid interactions. Such effects could be operative in lipid rafts that are known to segregate GPI-linked proteins (*9*, *32*).

In summary, the spin-label ESR, ^{31}P NMR, and DSC studies on the interaction of avidin with *N*-biotinyl-PEs presented here demonstrate that avidin binding can have a profound effect on the phase behavior of the lipids. Protein binding leads to a loss of lipid cooperativity and a restriction of the lipid chain mobility, in addition to triggering changes in the lipid polymorphism. In principle, such changes could effect transbilayer communication and facilitate internalization of ligands, in addition to modulating lateral communication mediated by the lipid chains at high protein binding densities.

ACKNOWLEDGMENT

We thank Frau B. Angerstein for her expert technical support in the lipid synthesis. We are extremely grateful to Dr. D. Riedel for performing the electron microscopy.

REFERENCES

1. Curatolo, W. (1987) *Biochim. Biophys. Acta 906*, 137−160.
2. Green, N. M. (1975) *Adv. Protein Chem. 29*, 85−113.
3. Wilchek, M., and Bayer, E. A. (1989) *Trends Biochem. Sci. 14*, 408−412.
4. Bayer, E. A., and Wilchek, M., Eds. (1990) *Methods Enzymol. 183*, Academic Press, San Diego, CA.
5. Bayer, E. A., Rivnay, B., and Skutelsky, E. (1979) *Biochim. Biophys. Acta 550*, 464−47.
6. Loughrey, H., Bally, M. B., and Cullis, P. (1987) *Biochim. Biophys. Acta 901*, 157−160.
7. Urdal, D. L., and Hakomori, S. (1980) *J. Biol. Chem. 255*, 10509−10516.
8. Lisanti, M. P., and Rodriguez-Boulan, E. (1990) *Trends Biochem. Sci. 15*, 113−118.
9. Simons, K., and Ikonen, E. (1997) *Nature 387*, 569−572.
10. Marsh, D., and Watts, A. (1982) in *Lipid−Protein Interactions* (Jost, P. C., and Griffith, O. H., Eds.) Vol. 2, pp 53−126, Wiley-Interscience, New York.
11. Lowry, O. H., Rosebrough, N. J., Farr, A. C., and Randall, R. J. (1951) *J. Biol. Chem. 193*, 265−275.
12. Rouser, G., Fleischer, S., and Yamamoto, A. (1970) *Lipids 5*, 494−496.
13. Swamy, M. J., and Marsh, D. (1994) *Biochemistry 33*, 11656−11663.
14. Swamy, M. J., Würz, U., and Marsh, D. (1993) *Biochemistry 32*, 9960−9967.
15. Blankenburg, R., Meller, P., Ringsdorf, H., and Salesse, C. (1989) *Biochemistry 28*, 8214−8221.
16. Aragarana, C. E., Kuntz, I. D., Birken, S., Axel, R., and Cantor, C. R. (1986) *Nucleic Acids Res. 14*, 1871−1882.
17. Hendrickson, W. A., Päler, A., Smith, J. L., Satow, Y., Merritt, E. A., and Phizackerley, R. P. (1989) *Proc. Natl. Acad. Sci. U.S.A. 86*, 2190−2194.
18. Weber, P. C., Ohlendorf, D. H., Wendeloski, J. J., and Salemme, F. R. (1989) *Science 243*, 85−88.
19. Pugliese, L., Coda, A., Malcovati, M., and Bolognesi, M. (1993) *J. Mol. Biol. 231*, 698−710.
20. Hemming, S. A., Bochkarev, A., Darst, S. A., Kornberg, R. D., Ala, P., Yang, D. S. C., and Edwards, A. M. (1995) *J. Mol. Biol. 246*, 308−316.
21. Darst, S. A., Ahlers, M., Meller, P. H., Kubalek, E. W., Blankenburg, R., Ribi, H. O., Ringsdorf, H., and Kornberg, R. D. (1991) *Biophys. J 59*, 387−396.
22. Swamy, M. J., and Marsh, D. (1997) *Biochemistry 36*, 7403−7407.
23. Arora, A., and Marsh, D. (1998) *Biophys. J. 75*, 2915−2922.
24. Boggs, J. M., and Rangaraj, G. (1985) *Biochim. Biophys. Acta 816*, 221−233.
25. Bartucci, R., Páli, T., and Marsh, D. (1993) *Biochemistry 32*, 274−281.
26. Cullis, P. R., and De Kruijff, B. (1979) *Biochim. Biophys. Acta 559*, 399−420.
27. Knowles, P. F., and Marsh, D. (1991) *Biochem. J. 274*, 625−641.
28. Sachse, J.-H., King, M. D., and Marsh, D. (1987) *J. Magn. Reson. 71*, 385−404.
29. Sharon, N. (1976) in *Mitogens in Immunobiology* (Oppenheim, J. J., and Rosenstreich, D. L., Eds.) pp 31−41, Academic Press, New York.
30. Hui, S.-W., and Sen, A. (1989) *Proc. Natl. Acad. Sci. U.S.A. 86*, 5825−5829.
31. Keller, S. L., Bezrukov, S. M., Gruner, S. M., Tate, M. W., Vodyanoy, I., and Parsegian, V. A. (1993) *Biophys. J. 65*, 23−27.
32. Simons, K., and Ikonen, E. (2000) *Science 290*, 1721−1726.

BI0029189